Title
Virtual manipulation of topography to test potential pool-riffle maintenance mechanisms

Journal
Geomorphology, 228

ISSN
0169555X

Authors
Jackson, James R
Pasternack, Gregory B
Wheaton, Joseph M

Publication Date
2015

DOI
10.1016/j.geomorph.2014.10.016

Peer reviewed

Virtual manipulation of topography to test potential pool–riffle maintenance mechanisms

J.R. Jackson[a], G.B. Pasternack[a]*, J.M. Wheaton[b]

[a]Department of Land, Air, and Water Resources, University of California at Davis, Davis, CA 95616-8628, USA

[b]Department of Watershed Sciences, Utah State University, Logan, UT 84322-5210, USA

*Corresponding author. Tel.: +1 530-754-9243; Fax: +1 530-752-5262;
E-mail: gpast@ucdavis.edu.

Abstract

In this study, numerical experimentation with two-dimensional hydraulic modeling of pool–riffle river topography drawing on the testbed data from the classic Keller (1971) study was used to investigate the effect of synthetically manipulating topography on the occurrence and magnitude of velocity and Shields stress reversals in a pool–riffle sequence. Reversals in velocity and shear stress have been used to explore mechanisms of pool–riffle maintenance, while Shields stress (a combined measure of transport capacity and substrate erodibility) is emerging in importance. The original site topography was modeled alongside six altered ones to evaluate the sensitivity of hydraulic reversals to subtle morphology — five incrementally wider pools and a filled pool. The Caamaño (2009) criterion, a simplified geometric threshold for predicting velocity reversals, was applied to each terrain to evaluate its utility. The original pool–riffle topography was just over the threshold for a velocity reversal and well over the threshold for a strong Shields stress reversal. Overall, pool widening caused a predominantly local response, with change to pool hydraulics and no change in section-averaged velocity in the riffle beyond the initial widening of 10%. Filling in the pool significantly increased the magnitude of reversals, whereas expanding it eliminated the occurrence of a reversal in mean velocity, though the Shields stress reversal persisted because of strong differentiation in bed material texture. Using Shields stress as a reversal parameter enabled the quantification of pool modification effects on pool–riffle resiliency. The Caamaño (2009) criterion accurately predicted reversal occurrence for the altered terrains with exaggerated effects, but failed to predict the weak reversal for the original topography. Two-dimensional modeling coupled with previously accepted hydrologic, geomorphic, and engineering analyses is vital in project design and evaluation prior to construction.

Keywords: velocity reversal; Shields stress; pool–riffle maintenance; fluvial geomorphology; 2D hydraulic modeling

1. Introduction

Characterizing mechanistic linkages between fluvial form and process is the central aim of research in fluvial geomorphology, while sustainably instilling such linkages in engineering designs remains a grand challenge in river rehabilitation. New tools are emerging to address these topics using a near-census approach — comprehensive, spatially explicit observation of the landscape emphasizing the ~ 1-m scale as the basic building block for characterizing geomorphic processes and ecological functions. For example, 0.01- to 1.0-m resolution remote sensing imagery and topographic mapping data sets (Hilldale and Raff, 2008; Marcus and Fonstad, 2008), spatially explicit topographic change detection (Wheaton, 2008; Milan et al., 2011; Carley et al., 2012), and 1-m resolution two-dimensional (2D) hydrodynamic modeling (Pasternack et al., 2006; Abu-Aly, 2013) are driving more detailed and accurate assessments of existing theories as well as the next generation of new ones. In this study numerical experimentation of pool–riffle channel topography from the classic Keller (1971) study on velocity reversal was done using 2D hydrodynamic modeling to investigate the role of subtle landform changes on the occurrence and magnitude of velocity and Shields stress reversals, with implications for understanding process–form linkages and using them in river rehabilitation.

Pool–riffle sequences are fundamental morphological features in moderate-gradient alluvial channels (Richards, 1976). Pools are low points in the bed topography with relatively low water surface slopes and finer bed material. Riffles are high points in the topography with relatively steep water surface slopes and coarser bed material

(Clifford and Richards, 1992). The role of pool–riffle relief in dictating the flow field is most significant under low flow conditions and becomes comparatively less pronounced as discharge rises (Cao et al., 2003; Brown and Pasternack, 2008). Meanwhile the understanding of pool–riffle dynamics has shifted over decades from a focus on relief (Keller, 1971) to relative wetted width between riffles and pools (MacWilliams et al., 2006; Sawyer et al., 2010). As an expression of interactive adjustments among hydraulics, bed scour, and sediment transport and deposition, pool–riffle sequences are responsible for generating a wide range of unique hydraulic patches that are critical in sustaining high-quality ecological niches necessary for diverse life history strategies by aquatic and riparian species (Woodsmith and Hassan, 2005; Moir and Pasternack, 2008; Pasternack and Senter, 2011). Enriching the understanding of pool–riffle hydrogeomorphic processes is therefore crucial to advancement of river science as well as rehabilitation and management of alluvial rivers.

1.1. Velocity reversal concept

Explanations for the maintenance of pool–riffle sequences have been debated for decades. Many studies rely on the velocity reversal hypothesis by Keller (1971) that sought to explain the areal sorting of bed material. Based on observations from one small creek in the Central Valley of California, the hypothesis states that ‘at low flow the bottom velocity is less in the pool than adjacent riffles’ and that ‘with increasing discharge the bottom velocity in pools increases faster than in riffles’ (Keller, 1971). At low flows, fine sediment is winnowed from riffles and deposited in downstream pools. At or near bankfull stages, flow velocity in pools is said to exceed the velocity over riffles. The shift in location of peak velocity maintains topographic relief of pool–riffle couplets; high flows scour sediment previously deposited in the pool, flow diverges out of the pool leading to deposition of larger sediment at the downstream riffle. While Keller's data showed that pool velocity increased faster than riffle velocity as discharge increased within the channel, it did not actually reveal the existence of a reversal in Dry Creek as no measurements of bankfull and above-bankfull conditions were made.

The velocity reversal hypothesis is controversial among the scientific community. Since its conception, many studies found velocity reversals in other river environments (Lisle, 1979; Jackson and Beschta, 1982), while others did not (Carling, 1991; Clifford and Richards, 1992). Uncertainty stems from the various parameters used to describe this phenomenon (Woodsmith and Hassan, 2005). Keller (1971) recorded near-bed velocities to support his hypothesis. Other field studies examined mean variables such as section-averaged velocity and shear stress (Clifford and Richards, 1992) or water surface gradient (Thompson et al., 1999). MacWilliams et al. (2006) organized past studies into a table and indicated whether they found a reversal or not. While past studies have included shear stress in their analyses, none have examined Shields stress as reversal parameter describing the maintenance of pool–riffle sequences.

Research continues to introduce alternative hypotheses for pool–riffle maintenance and to study more diverse settings. Building on the velocity reversal hypothesis and moving the focus to rivers whose alluvial landforms are highly forced by strong local outcrops, Thompson et al. (1999) proposed a model that incorporates flow-width constriction through a forced pool by recirculating eddies. Further field and laboratory studies examined interactions among discharge metrics, outcrop geometry, pool geometry, local hydraulics, and local morphodynamics in detail (Thompson and Hoffman, 2001; Thompson, 2002, 2006). The data collected by Woodsmith and Hassan (2005) did not indicate a reversal of mean velocity; to explain pool–riffle maintenance, these researchers suggested a conceptual model that combined mean bed shear stress and large-scale turbulent force. Similarly, MacVicar et al. (2010) examined forced pool–riffles and showed a reversal in near-bed velocity in the absence of a cross-sectional average reversal, pointing to localized turbulent forces. Notably, the ability of local turbulence to create near-bed hydraulic reversals in forced systems does not preclude the relevance of bulk hydraulic reversals. In forced settings, the onset of a bulk reversal could be a conservative estimate of when pool–riffle maintenance is beginning, and often river project designers seek high certainty of the presence of a key process.

MacWilliams et al. (2006) revisited Keller's field site, Dry Creek, and employed 2D and 3D numerical models to study the pool–riffle hydraulics. Both models predicted that a subtle velocity reversal took place on the pool–riffle sequence in Dry Creek, with the peak velocity occurring adjacent to the point bar and not over the deepest part of the pool by the outer cutbank. MacWilliams et al. (2006) indicated that the effects of lateral flow convergence resulting from a point-bar constriction and the routing of flow through the system were more significant in influencing pool–riffle morphology than the occurrence of a mean velocity reversal. Compatible ideas about the dominant role of width in pool–riffle maintenance (whether perceived in terms of channel, wetted, or ‘effective’ width) have grown in recent years (Repetto et al., 2002; Cao et al., 2003; Wu and Yeh, 2005; White et al., 2010).

In order to consolidate the findings of emerging research about the role of channel width on velocity reversals, Caamaño et al. (2009) proposed a highly simplified one-dimensional unifying criterion in which velocity reversal occurrence is a threshold function of the ratio of riffle to pool width, residual pool depth, and the depth of flow over a riffle. While much literature has focused on the existence of a single unifying hypothesis for the explanation of pool–riffle maintenance, the variability in support of these different hypotheses reflects the fact that different mechanisms may be at play in different circumstances, as evident in the citations earlier in this section. Indeed, the diversity in the literature now shows that no one mechanism governs all cases of pool and/or riffle maintenance, so studying each mechanism is important. This study provides new insights regarding hydraulic reversals, which are well established as one such maintenance mechanism and can be used by river practitioners in designing river rehabilitation projects (e.g., Wheaton et al., 2004, 2010; Brown et al., 2014).

1.2. Study objectives

In this study we experimented numerically with pool–riffle channel topography from the classic Keller (1971) study on velocity reversal using 2D hydraulic modeling to investigate the role of differences in width constrictions at the head of a pool on the occurrence and magnitude of velocity and Shields stress reversals, with implications for understanding process–form linkages and using them in river rehabilitation. The overall goal of this study was to refine the understanding of the role of width in pool–riffle maintenance by quantifying the flow-dependent sensitivity of reversals in velocity and Shields stress to systematic variations in wetted width at pools in gravel-bed channels with the aid of 2D hydrodynamic modeling. Considering only within bankfull flows, Cao et al. (2003) performed a numerical experimentation with a 2D hydrodynamic model. They showed that dramatic modifications to channel width could turn a bed shear stress reversal on or off. The question arises as to how sensitive the reversal mechanism is to incremental changes in channel geometry. By including overbank flows herein, a more comprehensive understanding of the system hydraulics was achieved.

We again returned to the pool–riffle couplet in Dry Creek near Winters, California that was mapped and monitored by Keller (1971), revisited by Keller and Florsheim (1993) in a 1D model study, and modeled in higher dimensions by MacWilliams et al. (2006). By using Keller's (1971) original Dry Creek study site as the starting topography for experimentation, it was possible to make new insights about the original hypothesis building on the reanalysis of MacWilliams et al. (2006). The use of Shields stress as a reversal parameter herein helped to describe the transport capacity specific to Dry Creek and yielded new discoveries about the transport regimes present that were previously missed for this case. In other settings, previous studies that included shear stress reversals did not relate the shear stress magnitude to substrate size. Contextualizing shear stress with river sediment size further strengthens the understanding of the process and thus the resiliency of the morphological units. In addition to testing for reversals, the Caamaño criterion was applied to each experimental topography during the analysis of 2D hydraulics to further evaluate the utility of that tool for use in pool–riffle evaluation and design. The results have significant implications for river science and management efforts because digital creation and testing of artificial fluvial terrain prior to project implementation can be used to avoid costly failures (Wheaton et al., 2004; Elkins et al., 2007; Brown and Pasternack, 2009; Pasternack and Brown, 2013).

2. Experimental methods

To assess the effect of pool geometry on velocity and Shields stress reversals and pool–riffle maintenance we (i) designed seven synthetic river digital elevation models (DEMs) with different pool-wetted widths and depths, (ii) conducted 2D modeling of the synthetic designs at five discharges ranging from 0.09 to 3.8 times bankfull (0.42 to 17.0 m^3/s), and (iii) extracted and compared performance indicators related to velocity and Shields stress reversal occurrence and magnitude to determine the hydraulic mechanism for each experimental terrain and implications for pool–riffle maintenance.

Previous studies have digitally modeled Dry Creek over this same flow range (Keller and Florsheim, 1993; MacWilliams et al., 2006) to examine pool–riffle hydraulics. The original DEM created by MacWilliams et al. (2006) and validated using field data from Keller (1969) was used in this study as the baseline terrain. Even though modeled flow exceeded the estimated bankfull discharge of the channel, this site is entrenched enough that the peak flow investigated was still contained within a well-defined channel and did not spread out over a floodplain. Hydraulic models tend to perform better at higher discharges than lower ones because higher momentum causes velocity vectors to straighten out; thus, the relation between depth and velocity switches from inverse to direct (Brown and Pasternack, 2008). Six experimental DEMs were made by manually altering the topography in the vicinity of the primary pool feature in AutoCAD 2002 Land Desktop. Cross-section–averaged velocity and Shields stress were the performance indicators used to evaluate each DEM for the occurrence and magnitude of the parameter reversals and pool–riffle maintenance.

2.1. Dry Creek study site

The riffle–pool–riffle sequence in Dry Creek in Winters, California (navigate to 38°31'43.72" N., 121°59'51.43" W. using Google Earth) is the classic field site from Keller's (1971) original velocity reversal hypothesis. Dry Creek is located in the eastern foothills of the California Coast Range, ~ 30 miles west of Sacramento. The site length modeled is ~ 135 m long and ~ 20-25 m wide. The upstream riffle is fairly uniform, with localized topographic highs across the channel at the riffle peak. The channel narrows upstream of the pool and the thalweg shifts to river right as the channel bends slightly to river left. The channel widens exiting the pool, two topographic high points exist downstream of the pool tail on river right. Downstream of the pool, the channel cross section becomes uniform and continues through the downstream riffle. Keller (1972) provided grain size distributions for the pool and riffle in Dry Creek; the median diameter was 10 mm at the pool, 32 mm on the adjacent point bar, and 32 mm at the downstream riffle. Together with morphological controls, this size differential enhances the potential for different scour regimes for these morphological units. Analyses of the 2D model results herein focus on cross sections of the pool and downstream riffle, consistent with past studies.

2.2. Experimental terrains

The numerical experimentation in this study involved manipulating the DEM of Dry Creek that MacWilliams et al. (2006) made by digitizing the contour map plate in Keller (1969). The primary focus of this study involved assessing width expansions to see when and if the existent flow-dependent reversals might be lost. No further width constrictions were tested because the original channel was constricted and already exhibited velocity and Shields stress reversals in the base case, so further width constriction would simply strengthen that. In contrast, how much wider the channel needed to be in order for the reversals to disappear was unknown. This is of critical importance in geomorphology and river engineering because empirical channel design specifies design width on the basis of bankfull width predicted using regional regression relations (e.g., Osterkamp et al., 1983; Williams, 1986; Xu, 2004) that have significant deviations between width at a real site and the regression best-fit value. If the error in width specification exceeds that to maintain the process of flow convergence routing, then geomorphic dynamics may cause the as-built landforms to fall apart. By testing different expansions, it was possible to determine not only the width deviation for the velocity reversal to disappear but also evaluate the effectiveness of the 1D Caamaño criterion at the same time. In addition, a reference scenario with no pool present at all was made to investigate the potential for the onset of pool formation as a result of flow-dependent scour at the pool location had the pool not been there at the outset, but with the natural constriction at that location. Virtual pool filling has also been tested by Biron et al. (2012). Thus the totality of the experimental design of this study involved exploring the range of reversal strengths and the implications of those for pool–riffle maintenance using six topographic scenarios.

The base case used for comparison was the original Dry Creek (DC) DEM. The first experimental terrain, 'No Pool' (NP), consisted of the pool filled in to a minimum elevation of 26.5 m, corresponding with the downstream riffle thalweg elevation, thereby erasing the pool from the terrain. For the remaining five experimental terrains, width expansions of ~ 10, 15, 20, 25, and 30% (correspondingly named WE10, … WE30) were applied to the original pool feature by excavating the point bar and adjacent bank material. The pool width was first expanded by 30 percent where the pool XS station line intersects the 26.8 m (88 foot) contour, and the remaining designs were created incrementally. A width change of just 5% was found to be so subtle compared to the original topography that it was not investigated. A planview comparison of the DC, NP, WE10, and WE30 terrains is shown in Fig. 1, while the pool cross section for all terrains is shown in Fig. 2. A summary of the widths and cross-sectional areas associated with the original pool morphology, no pool, and width-expanded designs is presented in Table 1. Model results from this range of pool–riffle width and depth ratios were used to assess the hydraulic mechanism for each terrain, how much the pool feature in Dry

Creek must be widened before it no longer exhibited a velocity or Shields stress reversal, and the capacity of the pool–riffle sequence to self-maintain.

2.3. 2D FESWMS model

A 2D hydrodynamic model, Finite Element Surface Water Modeling System 3.1.5 (FESWMS), was used to simulate hydrodynamics for the baseline channel and the alternative terrains. This model was previously validated for use in shallow, gravel-bed rivers many times (e.g., examples from four different rivers are available in Pasternack et al., 2006; Brown and Pasternack, 2008; Mainwaring et al., 2009; and Sawyer et al., 2010). The FESWMS model of Keller's (1971) Dry Creek site was previously developed, validated, compared to 1D and 3D models, peer-reviewed, and published by MacWilliams et al. (2006). This study applies the preexisting model to experimental terrains in the fashion of previous studies by Cao et al. (2003), Pasternack et al. (2004, 2008), and Pasternack and Brown (2013).

Here the essential features of the model are summarized and the reader is referred to MacWilliams et al. (2006) for complete details. The FESWMS model used a finite element mesh (hybrid of triangular and quadrilateral elements) with a roughly uniform node spacing of 0.45 m. The elevation at each node was interpolated from the triangulated irregular network (TIN) DEM of the site. A constant eddy viscosity value of 0.027 m^2/s was used for all model runs.

Earlier studies explained roughness parameterization, but primarily addressed the decision to not spatially distribute roughness parameter values and did not explain the effect of discharge on roughness. Classic parameterization of channel roughness for analytical methods and 1D hydraulic models involves consideration of many potential form roughness contributors that vary with discharge. In contrast, 2D models explicitly resolve many scales of form roughness, and thus parameterization is required only for unresolved, sub-grid-scale features (e.g., grains, grain heterogeneity, grain clusters, potential bank roughness where flow interacts with a steep bank composed of different material than the bed, and unresolved bed topography for unvegetated alluvial channels). Notably, because the channel in this study is entrenched, higher flows do not spill out onto a floodplain at all; they modestly expand onto the point bar and higher up the steep bank — both of which are composed of the same material as the bed. Our past experience with 2D modeling of floods in gravel-bed rivers and bedrock canyons for which extensive water surface elevation data was available to calibrate flow-dependent Manning's N showed no decrease in Manning's N with increasing discharge in this setting— the best-performing parameter value can change up or down and no apparent control or trend is associated with the discharge. This happens because water surface elevation is an integrated measure of roughness; any local reduction in Manning's N resulting from the increased relative submergence in the thalweg is offset by form roughness associated with increasingly inundated topographic features as well as the addition of new roughness elements along the banks that have extremely low relative submergence. Abu-Aly et al. (2013) provide strong evidence of this phenomenon for 2D modeling of vegetated channels. To assess local roughness at the same scale as needed in the model, one would need detailed velocity observations.

Because collecting data during floods is hazardous, the scientific literature is bereft of cases in which velocity data is used to validate the performance of 2D models during overbank floods. Lacking high quality, unique calibration of Manning's N for each overbank flow, this study of a classic data set has to be recognized as in the realm of scientific exploration and not predictive forecasting with high certainty for the purpose of critical management decision making, using the uncertainty concepts of Murray (2003). In a real-world application of the methods and ideas in this study, river rehabilitation designers and modelers should thoroughly calibrate and validate their study sites using modern methods (Pasternack, 2011). Thus, in keeping with validated 2D and 3D hydrodynamic models of the site reported by MacWilliams et al. (2006) for the same flow range used in this study, a uniform bed roughness Manning's N of 0.041 was used.

Keller's original field measurements (1969, 1971) were made at discharges of 0.42, 0.97, and 4.5 m^3/s, with this last being close to bankfull discharge. The HEC-RAS model simulations by Keller and Florsheim (1993) were conducted for five steady flow rates including the three discharges measured by Keller and two larger discharges of 8.5 and 17 m^3/s. These five steady flows ranging from 0.09 to 3.8 times bankfull were modeled in FESWMS in this study for all terrains.

2.4. Experimental test variables

The comparison of hydraulic mechanisms driving pool–riffle maintenance at the study site was made using velocity and Shields stress as the test variables. FESWMS hydraulic predictions include depth and velocity magnitude scalars at each computational mesh node. Using the workflow in Pasternack (2011) and ArcMap 10.1, velocity magnitude and depth TINs were generated and then converted into rasters. For each scenario and discharge simulated, cross-sectional velocity profiles at the pool and downstream riffle were extracted from each TIN at 0.5-m spacing along station lines in ArcGIS.

Different field methods and theoretical approaches to estimating bottom-boundary shear stress yield significantly different numbers (Whiting and Dietrich, 1991; Wilcock et al., 1996; Smart, 1999). Traditional approaches that use whole-column velocity observational data at a point to estimate bottom-boundary shear stress have been found to match predictions made using point-scale, depth-averaged velocity outputs from a 2D model (Pasternack et al., 2006). Traditional approaches that estimate shear stress using velocity measurements right above the riverbed yield numbers significantly smaller than those using whole-column measurements, even though they are supposed to be estimating the same point-scale phenomenon. Making measurements near the bed that can be used to estimate shear stress is also highly fraught with uncertainty because of the presence of heterogeneous grain clusters and complex microhydraulics (Buffin-Belanger and Roy, 1998). Pasternack et al. (2006) found that if one wants to obtain 2D model predictions of shear stress matching values estimated from near-bed velocity measurements, then one can multiply 2D model shear stress output by 0.51 (essentially a factor of one-half). MacWilliams et al. (2006) reported the same scaling factor for converting 2D model shear stress output to match near-bed shear stress outputs from a 3D model. However, it is unclear if that is really warranted as width-scale spatial patterns of geomorphic change during flows many times bankfull discharge require width-scale, spatially coherent patches of shear stress, not just what happens to one grain at the tip of a velocity sensor. For example, Sawyer et al. (2010) compared the depth-averaged shear stress output from a 2D model to actual channel change in a gravel/cobble river for a flood of ~ 7.6 times bankfull discharge. They found that this variable was successful at differentiating coherent regions of scour and deposition associated with processes such as island deposition, knickpoint scour, pool scour, and floodplain deposition, but no point-by-point correlation between shear stress and elevation change existed. Instead, unresolved local factors controlled point-scale changes. Thus, the depth-averaged shear stress output from a 2D model ought to be capable of identifying coherent regions susceptible to geomorphic change associated with flow convergence routing even if it cannot precisely predict the point-scale shear stress at any location with real-world sub-grid-scale complexity.

Shields stress was calculated at station points along the pool and downstream riffle using the profiles of local depth and velocity extracted from the FESWMS results, *not* calculated from the section-averaged depth and velocity. This was accomplished by employing the drag force method (Pasternack et al., 2006):

$$C_D = (32.2n^2) / [2.208(H^{1/3})] \quad (1)$$

$$\tau_v^{\,b} = 1.937 C_D V^2 \quad (2)$$

$$\text{and } \tau^* = \tau_v^{\,b} / [(\gamma_s - \gamma_w) d_{50}] \quad (3)$$

where C_D is the drag coefficient, n is the Manning's roughness factor, H is water depth (m), $\tau_v^{\,b}$ is bed shear stress in the direction of the velocity vector V (m^2/s), τ^* is Shields stress, γ_s is sediment specific weight, γ_w is water specific weight, and d_{50} is median grain size. Median grain sizes were extracted from the frequency distributions of bed material at the pool and riffle provided by Keller (1972) and are mentioned in section 2.1 above. Shields stress was used to compare the synthetic designs against the original with respect to sediment transport capacity and resilience of the pool–riffle couplet (Pasternack, 2011).

Note that if the local grain size at any arbitrary location were to be known to be higher than the surrounding terrain and roughness was raised there accordingly in Eqs. (1-3), then it would appear to increase Shields stress. However, if the effect is also natively instituted into the 2D hydraulic model then it would also lower velocity and slightly raise depth. Because the velocity effect in Eqs. (1-3) is nonlinear, it might outweigh the drag coefficient and depth effects, causing a decrease in Shields stress. The key point is that one cannot easily discern how simple adjustments to boundary conditions will effect the nonlinear physics, which is why 2D modeling is useful. In this study we chose to stay as true as possible to past model setups for the site and just vary grain size in Eq. (3) where we had data from the original field work by Keller (1972). In modern practice, bed material facies can be mapped for baseline studies and specified as part of project designs, eliminating the deficiency we faced in our scientific exploration of an important historical data set.

Lisle et al. (2000) defined sediment transport regimes relative to τ^* as $\tau^* < 0.01$ represents no transport; $0.01 < \tau^* < 0.03$ represents probabilistically intermittent entrainment; $0.03 < \tau^* < 0.06$ represents partial transport; $0.06 < \tau^* < 0.1$ represents full transport of a ‘carpet’ of sediment 1-2·D_{90} thick, and 0.1 < τ* corresponds with potentially channel-altering conditions. These threshold delineations have uncertainty but provide a reasonable basis for characterizing and comparing sediment transport conditions (Sawyer et al., 2010). Using these bins, sediment transport regimes were generated at the pool and downstream riffle cross sections over the range of discharges simulated to examine the relative resiliency of each terrain.

2.5. Determination of test outcomes

2.5.1. Reversal testing

A velocity reversal refers to the discharge at which the cross-sectional average velocity at the pool exceeds the cross-sectional average velocity at the riffle (MacWilliams et al., 2006). To test for the occurrence and magnitude of a velocity reversal, at-a-station velocity-versus-discharge curves were generated for each scenario from the profiles described in section 2.4. Velocity profiles at the pool and downstream riffle were averaged for each scenario and plotted for the five flows simulated. The resulting figures show that a reversal was achieved if the average velocity-versus-discharge curve at the pool cross section surpassed that at the riffle within the flows simulated. The strength of the reversal was identified by the relative exceedence of the pool velocities to the riffle velocities in the 17 m^3/s simulation.

The evaluation of cross-sectional average Shields stress (τ_{xs}*) reversal occurrence and magnitude followed the same method as the velocity reversals. Average Shields stress-versus-discharge curves at the pool and riffle cross sections were plotted against one another for each design. The occurrence and magnitude were determined by whether the pool curve exceeded the riffle curve and by how much it dominated in the 17-m^3/s simulation.

2.5.2. Sediment transport regime testing

Past studies in Dry Creek did not include Shields stress analyses of pool–riffle couplets, so transport regimes were not previously quantified. Understanding the resiliency of morphological units requires comparison of hydraulics and local substrate. Sediment data available for Dry Creek was limited; Keller (1971) provided grain size distributions for the pool and riffle but comprehensive substrate maps of this pool–riffle couplet do not exist. Shields stresses were therefore only calculated along the cross sections of the pool and riffle for analysis. These cross-sectional representations of the pool–riffle couplet were thought sufficient in characterizing the transport capacity of the site for the purposes of this study. Note the variable of concern for sediment transport regime testing is Shields stress (τ^*) along the pool and riffle cross section opposed to cross-sectional mean Shields stress (τ_{xs}^*) used for reversal testing.

The statistical distributions of Shields stress bins for $0.01 < \tau^* < 0.03$ (intermittent transport), $0.03 < \tau^* < 0.06$ (partial transport), $0.06 < \tau^* < 0.1$ (full transport), and $0.1 < \tau^*$ (channel altering) were used to analyze the relative resilience of the alternate designs across the range of discharges simulated. By comparing the τ^* distributions of each modified design with the original Dry Creek along with τ_{xs}^*, changes in transport competence and expected resilience were determined. Because the original Dry Creek pool–riffle couplet persisted naturally over the range of flows explored in this study, it was used as the base for comparison.

2.5.3. Caamaño criterion

In order to consolidate the results of previous studies on velocity reversals, Caamaño et al. (2009) developed a simplified criterion aimed to predict whether a pool–riffle couplet would exhibit a reversal. Caamaño et al. (2009) corroborated the criterion with data from previous studies using a simplified version of the model that neglected expansion and frictional head losses and cross-sectional shape ratio. The resulting velocity reversal threshold is given by

$$(B_r / B_p) - 1 = D_z / h_{Rt} \quad (4)$$

where B_r and B_p are riffle and pool water surface widths, respectively; D_z is residual pool depth; and h_{Rt} is riffle thalweg depth. These parameters were obtained for each model herein at 17.0 m^3/s to apply the criterion to the flow wherein a maximum hydraulic reversal would exist. If the criterion fails here, it certainly fails at lower discharges. Consistent with Caamaño, the criterion was applied to the pool and downstream riffle.

The accuracy of the Caamaño criterion prediction has been called into question by MacVicar et al. (2010) for the case of forced pools because it lacks consideration of local turbulence near the bed. This study provided an opportunity to investigate it on a larger, subwidth scale basis and where the constricting point bar is alluvial and incrementally removed. The criterion was tested by first evaluating whether each scenario actually exhibited a velocity reversal or not. For the real DC terrain, strong field evidence for a velocity reversal as well as supporting evidence for its occurrence based on 1D, 2D, and 3D models existed (Keller and Florsheim, 1993; MacWilliams et al., 2006). If the Caamaño criterion predicted the presence of a velocity reversal and it was not in fact present in the 2D model or vice versa, then the simplifications and assumptions of the criterion used would turn out to be not reliable, even limiting the evaluation to just bulk hydraulic phenomena and not considering microscale turbulence processes affecting individual grains.

3. Results

3.1. Hydraulics

A complete comparison of FEWSMS-predicted depths and velocities at the pool and riffle is shown in Table 2. Depth-averaged velocity maps of the highest and lowest (0.42 and 17.0 m^3/s) discharges illuminate the hydraulic mechanisms behind each scenario (Figs. 3, 4). The WE15, WE20, and WE25 results were omitted for conciseness.

Topographically filling the pool increased velocities at the pool and riffle for all flows. For NP at 0.42 m^3/s, mean velocity at the pool increased by 0.06 m/s (48%). The vertical constriction in flow imposed by filling the pool was less of a factor at greater discharges but still amplified flow convergence through the pool; mean velocity was 0.12 m/s (10%) greater than DC at 17 m^3/s. Mean velocity at the riffle increased by 0.02 m/s (8%) for the low flow of 0.42 m^3/s. At 17 m^3/s, no difference in mean riffle velocity between DC and NP scenarios was predicted.

As with the NP scenario, the effects of pool modification on system hydraulics were mostly localized at the pool for the WE scenarios. Overall, velocities decreased throughout the site for the first width expansion with the exception of at the riffle. Only mean pool velocity consistently dropped with subsequent pool expansions. At 0.42 m^3/s, no change was seen at the pool for the first two width expansions, but mean velocity dropped 7% for WE20 and was down 14% for WE30. Mean riffle velocity remained unchanged for all pool expansions at the low flow. Mean pool velocities continued to decrease with increasing discharge, but to a lesser degree. The intermediate discharges simulated yielded interesting results at the riffle. Compared to DC, the mean riffle velocities for WE20 through WE30 were actually greater at 0.96 and 4.5 m^3/s, whereas WE10 and WE15 were lower than DC. At 8.5 and 17 m^3/s, all width expansions yielded lower riffle velocities.

3.2. Reversal test results

At-a-station velocity versus discharge plots showed that the pool–riffle couplet is naturally at the cusp of having a mean velocity reversal (Fig. 5). Even a 10% increase in pool width would turn off the mechanism. For the real-world base case, FESWMS predicted a mean velocity reversal in Dry Creek at a discharge between 6 and 7 m^3/s (~ 130 and 160% of bankfull). The predicted mean pool velocity in Dry Creek was only 5.6% greater than mean downstream riffle velocity at 17 m^3/s. For the NP case, FESWMS predicted a velocity reversal at a discharge just below 3 m^3/s (67% of bankfull). The mean velocity was 12% greater at the pool than the riffle at 17 m^3/s, which is a significant strengthening of the reversal because of the absence of a pool. No velocity reversals were predicted for any of the width expansion topographies; mean velocity at the downstream riffle was always greatest. Mean pool velocity for width expansions WE10 and WE30 were respectively 12 to 15% less than the riffle velocities at 17 m^3/s.

In contrast to the mean velocity reversal, the τ_{xs}* reversal showed a dramatically different flow dependence, with a much lower discharge and greater resilience against width expansion (Table 3, Fig. 5). Reversals in Shields stress occurred for all terrains except for NP, in which pool τ_{xs}* was always greater than the downstream riffle, emphasizing a strong propensity for pool scour and substrate coarsening at greater discharges.

At 0.42 m^3/s, the WE scenarios had the same τ_{xs}* as DC: 0.003 in the pool and 0.006 at the downstream riffle. A reversal in τ_{xs}* was predicted just below 0.96 m^3/s for the DC terrain. At 17 m^3/s, DC τ_{xs}* in the pool was about 3.5 times higher than in the riffle. Pool τ_{xs}* dominated at all flows for the NP design; pool τ_{xs}* was slightly greater than that of the riffle at 0.42 m^3/s and over four times that of the riffle at 17 m^3/s. For the WE10 design, the τ_{xs}* reversal was predicted just above the 0.96 m^3/s discharge, which was at a slightly higher stage than for DC. The reversal was predicted to occur at 1.3 m^3/s for WE30. Pool τ_{xs}* for WE30 was only twice that of the downstream riffle at 17 m^3/s.

3.3. Sediment transport regime analysis

Overall, pool filling caused an increase in τ^*, while widening the pool reduced τ^*. Again, the effects were prominent over the pool and less pronounced over the riffle. At 0.42 m^3/s, τ^* statistics were difficult to distinguish (Fig. 6A). Only NP exhibited τ^* in the intermittent transport range (28% of the cross section), and no transport was predicted for DC and WE scenarios. The fraction of the riffle cross section with τ^* in the partial transport range was 24% for DC, 28% for NP, and 11% for WE scenarios.

Results for the intermediate flows clearly reveal changes in the sediment transport regime caused by pool alteration. At 4.5 m^3/s, 31% of pool τ^* values were above the 0.1 threshold for channel altering conditions for the NP terrain (Fig. 6C). The fraction of pool with τ^* in the full transport range dropped from 60% in DC to 28% in WE10; it fell to 0% by WE20. The effects of widening were less apparent at the riffle; 21% full transport for DC was reduced to 19% at WE10 and declined to 16% for WE30.

At 17 m^3/s, pool τ^* dominated for all terrains (Fig. 6E). Dry Creek exhibited 89% channel-altering values that increased to 100% for NP. Pool widening decreased the pool fraction of channel altering τ^* to 70% for WE10 and 60% for WE30. Full transport was predicted at 23% of the DC riffle. Full transport on the riffle reduced to 15% for NP, and the WE terrains ranged from 21% (WE10) to 15% (WE30).

3.4. Caamaño criterion

The Caamaño criterion was applied to all scenarios to predict whether any would experience a velocity reversal (Fig. 7). The criterion correctly predicts a mean velocity reversal in the NP design but misses the reversal that occurs naturally in the real DC terrain. The absence of a mean velocity reversal in each WE design is correctly captured by the Caamaño criterion. Because the Caamaño criterion does not account for sediment, it cannot predict the occurrence of a τ_{xs}* reversal, which is present in all terrains using the natural bed materials at the site. The inability to incorporate sediment transport is a significant limitation of the tool.

4. Discussion

4.1. Hydraulics

A key finding in the pool geometry experiments was that the changes to the width constriction and pool geometry affected the hydraulics in the pool region to a much greater extent than the riffle region, though it did influence both. For example, filling the pool increased mean pool velocity by 17% at 8.5 m^3/s but only increased mean riffle velocity by 1%. At the same discharge, mean velocity for WE20 was 21% lower than that for DC at the pool but only 1% lower than that for DC at the riffle.

Because flow convergence routing (e.g., MacWilliams et al., 2006) kicks in at higher discharges, mean velocity on the riffle was only affected at higher discharges for the WE scenarios. Mean velocities at the riffle were unchanged by pool expansions during the 0.42 m^3/s discharge. At the intermediate discharges 0.96 and 4.5 m^3/s, riffle hydraulics changed with expansions. The first two expansions (WE10 and WE15) resulted in lower velocities at the riffle compared to DC, while greater pool expansions (WE20 through WE30) resulted in slightly higher riffle mean velocities. Mean riffle velocity decreased with the first pool expansion during the 8.5 and 17.0 m^3/s discharges but exhibited negligible change with additional expansions.

By expanding the pool by just 10% of the original width, the flow convergence that originally took place at high discharges was significantly reduced. The riffle became the constricting feature in this sequence after the width constriction was widened by 20% and beyond. The physical extent of the pool expansions did not extend to the riffle so velocities at the riffle did not change significantly with further expansions once flow convergence was eliminated at the pool. Nonetheless, expanding the pool reverses the hydraulic character that was considered to maintain the pool–riffle sequence during high flow events.

4.2. Reversals

The original pool–riffle sequence in Dry Creek is just beyond the fringe of exhibiting a velocity reversal and is thus sensitive to changes in pool geometry. Filling in the deepest areas of the pool reduced the cross-sectional area and resulted in higher pool velocities at all flows and a stronger mean velocity reversal. Because of the increased flow convergence, the jet of flow exiting the pool in the NP design resulted in a slight increase in downstream riffle velocities at all discharges simulated. Because the DC geometry is in a near-critical state, widening the pool by 10% eliminated the occurrence of a mean velocity reversal. Each additional expansion created a greater bankfull differential in velocity in favor of riffle scour, a condition that can lead to degradation of the pool–riffle system by the reverse domino mechanism of Pasternack et al. (2008).

The results for mean Shields stress reversal were vastly different than velocity. A reversal in Shields stress was predicted to take place just below 0.96 m^3/s for the DC terrain compared to about 6.5 m^3/s for the velocity reversal. Filling the pool led to greater $\tau_{xs}*$ in the pool always, and the strong $\tau_{xs}*$ reversal occurring in DC was only slightly reduced by expanding the pool, not eliminated. Both variables shed light on hydraulic mechanisms, but this study shows that future research should further pursue Shields stress.

Obtaining substrate data and facies maps comprehensively for long segments of rivers is challenging, but emerging technologies are resolving that problem for subaerial terrain (Carbonneau et al., 2006) and may eventually address subaqueous terrain (e.g., multibeam SONAR surveys). In the near-term, rapid facies mapping of subaerial and subaqueous substrate with visual estimation of the percent abundance of discrete size fractions has been found to capture reach- and morphological-unit-scale relations between hydraulics and grain size metrics (Buffington and Montgomery, 1999; Jackson et al., 2013) as well as to be useful for 2D hydraulic modeling and Chinook salmon (*Onocorhynchus tshawytscha*) spawning microhabitat prediction (Pasternack et al., 2013). Meanwhile, centimeter-scale digital color imagery of subaerial alluvium can readily be used to make facies maps, and then size metrics for each facies polygon can be obtained using emerging algorithms (e.g., Warrick et al., 2009; Buscombe et al., 2010; Bertoldi et al., 2012; Nelson et al., in press). Ground-based Light Detection and

Ranging (LiDAR) can directly resolve the dimensions of individual subaerial grains (Brasington et al., 2012) and Airborne LiDAR can be used to derive surface roughness maps of subaerial terrain.

4.3. Sediment transport regime

Comparing scenarios using τ_{xs}* showed little to no change at the riffle after the initial pool width expansion (WE10). Riffle velocity and τ_{xs}* remained unchanged with additional expansions. When classified into bins based on sediment transport regimes of Lisle et al. (2000), τ* showed a trend in its distribution across the riffle. Widening the pool incrementally shifted the sediment transport regime toward less transport at the pool and riffle, although changes at the riffle were less pronounced. This effect was more apparent at higher discharges. At 0.42 and 0.96 m^3/s, no transport or intermittent transport was predicted at the pool and riffle (Figs. 6A, B). At 4.5 m^3/s, the majority of the pool entered full and partial transport for DC (Fig. 6C). Here, the effect of pool alterations was revealed through τ* bins. Pool filling raised 31% of the pool cross section above the channel-altering threshold; while the fraction of pool τ* in full transport was incrementally reduced in WE10 and WE15, and then eliminated in WE20. This trend was evident in the channel-altering bins at 8.5 m^3/s; the fraction of channel-altering τ* was absent in WE15. Comparing averaged τ* values used for the reversal analysis does not capture the underlying trends in τ* distributions for the terrains, which is an important indicator of the importance of a spatially explicit approach to simulating and assessing hydraulic scour mechanisms.

To further understand the sediment transport regimes inferred with the classification scheme of Lisle et al. (2000), flow frequency and duration is needed. Historic hydrologic data is not available for Dry Creek, so the significance of the modeled flows in terms of their ability to change landforms is uncertain. Grain sizes used in this analysis significantly contributed to the differences in τ^* between pool and riffle. As discharge approaches 17 m^3/s, width undulations have less influence and the whole channel trends toward full transport. To determine the importance of full transport, one should know how often 17 m^3/s occurs and for what duration. This is a limitation of using a historic site; future studies at modern sites could likely answer this question. For example, Sawyer et al. (2010) found that a flood on a gravel/cobble bed river with overbank flow for 14 days and an instantaneous peak of 7.7 times bankfull discharge exhibited a velocity reversal and caused rejuvenation in pool–riffle relief along with other substantial morphological changes.

4.4. Caamaño criterion

One of the secondary objectives of this study was to apply the Caamaño criterion to each modification and determine its accuracy as a guide to practitioners. Caamaño et al. (2009) noted that the criterion 'does not account for the spatial and temporal variation of local (point) velocity reversal'. Thus, weak, local, or transient reversals may not be accurately predicted with the simplified one-dimensional criterion. The velocity reversal predicted for the original topography in Dry Creek was weak and the Caamaño criterion failed to predict its occurrence. The criterion more accurately predicts reversal occurrence or lack thereof for the altered terrains in which the pool is either filled or expanded. Filling the pool reduces the residual pool depth relative to the riffle thalweg and a velocity reversal will more likely occur (Caamaño et al., 2009). The criterion successfully predicts a reversal for the filled pool. Pool width must be less than riffle width for a cross-sectional average velocity reversal to occur. Expanding the pool resulted in widths greater than the riffle at the largest discharge and the resulting absence of velocity reversals was accurately predicted by the Caamaño criterion. While attractive for its simplicity, the Caamaño criterion cannot predict near-bed or peak velocity reversals, which MacVicar et al. (2010) have shown to occur in forced pools in the absence of an average velocity reversal. This reminds us that pool formation and maintenance can be attributed to different mechanisms in different settings and that the criterion may not be applicable in all cases. However, where the channel configuration matches the assumptions of the method and it does predict a velocity reversal, one will likely occur and play an important role in pool–riffle maintenance. Because the Caamaño criterion does not account for sediment, it cannot predict the τ_{xs}* reversals that took place in all terrains. An opportunity exists to create a new criterion to solve that problem, but given that 2D models provide a breadth of utility in geomorphic and ecohydraulic assessment (Pasternack, 2011) as well as river restoration design (Pasternack et al., 2004; Brown and Pasternack, 2009; Pasternack and Brown, 2013), getting the best available answer with a spatially explicit representation of hydrogeomorphic processes makes more sense than accepting risk and liability associated with a simplified metric. Given typical project construction documents and associated engineering/geomorphic analyses, the effort to make and evaluate 2D models is actually quite small.

5. Conclusions

In this study the historic pool–riffle couplet analyzed by Keller (1971) was once again revisited and used in a systematic experiment to assess the sensitivity of velocity and Shields stress reversals to incremental topographic changes and to test the Caamaño criterion to aid practitioners considering using it for engineering design. This time synthetic terrains were made, not unlike river engineering designs, in which the constriction at the pool was incrementally removed. For contrast we included one case in which the pool was filled in. Depth and depth-averaged velocity for each terrain at five discharges from base flow to overbank flood were predicted with a preexisting, validated 2D model of the site and combined with historic substrate measurements to reveal hydraulic mechanisms, including velocity and Shields stress reversals. Removing the width constriction was found to shut down the velocity reversal because it was already weak in the baseline terrain. However, it did not shutdown the Shields stress reversal because the difference in bed material grain size between the pool and riffle was too large. That points to the other important discovery in this study: by accounting for substrate composition, Shields stress exhibited a different mechanism than velocity, though obviously related to velocity as given in the governing equation. This study investigated a simple setting with relatively limited data compared to what modern data sets are getting, so limited spatial variation is present. Nevertheless, characterizing the sediment transport regime for modern data sets with ranges of Shields stress will be an effective way to introduce channel bed erodibility into spatially explicit models of scour potential without having to add full morphodynamics to a model. Finally, the Caamaño criterion can be used in geomorphic assessment and design only when the velocity reversal is very strong. The criterion cannot account for peak reversals, which is mentioned by Caamaño (2009) and remains the main criticism of the unifying one-dimensional criterion for velocity reversals and pool–riffle maintenance (MacVicar et al., 2010). Also, the Caamaño criterion cannot account for Shields stress reversals. Explicit 2D modeling of complex landforms has many benefits for channel assessment and design and is becoming increasingly affordable and simple to implement. Nevertheless, the Caamaño criterion has already proven useful for preliminary design development and testing in the early stage of developing terrain alternatives before it makes sense to do 2D modeling.

Acknowledgements

This project was largely done on an independent basis by the authors with no direct financial support. Indirect financial support for this project was provided in the form of general salary contributions to Prof. Pasternack by the USDA National Institute of Food and Agriculture, Hatch project number #CA-D-LAW-7034-H. We thank four anonymous reviewers for helpful reviews of the manuscript that guided revision and editor Richard Marston for a thorough editor's markup.

References

Abu-Aly, T.R., Pasternack, G.B., Wyrick, J.R., Barker, R., Massa, D., Johnson, T., 2013. Effects of LiDAR-derided, spatially-distributed vegetative roughness on 2D hydraulics in a gravel–cobble river at flows of 0.2 to 20 times bankfull. Geomorphology, doi:10.1016/j.geomorph.2013.10.017.

Bertoldi, W., Piégay, H., Buffin-Bélanger, T., Graham, D., Rice, S., 2012. Applications of Close-Range Imagery in River Research. In: Carbonneau, P.E. and Piégay, H. (Eds.), Fluvial Remote Sensing for Science and Management. John Wiley and Sons, Ltd., Chichester, UK. doi:10.1002/9781119940791.ch15.

Biron, P.M., Carver, R.B., Carré, D.M., 2012. Sediment transport and flow dynamics around a restored pool in a fish habitat rehabilitation project: Field and 3D numerical modeling experiments. River Research and Applications 28, 926-939.

Brasington, J., Vericat, D., Rychkov, I., 2012. Modeling river bed morphology, roughness and surface sedimentology using high resolution terrestrial laser scanning. Water Resources Research 48, W11519. doi:10.1029/2012WR012223.

Brown, R.A., Pasternack, G.B., 2008. Engineered channel controls limiting spawning habitat rehabilitation success on regulated gravel-bed rivers. Geomorphology 97, 631-654.

Brown, R.A., Pasternack, G.B., 2009. Comparison of methods for analyzing salmon habitat rehabilitation designs for regulated rivers. River Research and Applications 25, 745-772.

Brown, R.A., Pasternack, G.B., Wallendar, W.W., 2014. Synthetic river valleys: creating prescribed topography for form–process inquiry and river rehabilitation design. Geomorphology 214, 40-55. 10.1016/j.geomorph.2014.02.025.

Buffin-Belanger, T., Roy, A.G., 1998. Effects of a pebble cluster on the turbulent structure of a depth-limited flow in a gravel-bed river. Geomorphology 25(3-4), 249-267.

Buffington, J.M., Montgomery, D.R., 1999. A Procedure for classifying textural facies in gravel-bed rivers. Water Resources Research 35(6), 1903-1914. doi:10.1029/1999WR900041.

Buscombe, D., Rubin, D.M., Warrick, J.A., 2010. A universal approximation of grain size from images of noncohesive sediment. Journal of Geophysical Research Earth Surface 115, F02015. doi:10.1029/2009JF001477.

Caamaño, D., Goodwin, P., Buffington, J.M., Liou, J.C., Daley-Laursen, S., 2009. Unifying criterion for the velocity reversal hypothesis in gravel-bed rivers. Journal of Hydraulic Engineering 135(1), 66-70. doi:10.1061/(ASCE)0733-9429(2009)135:1(66).

Cao, Z., Carling, P., Oakey, R., 2003. Flow reversal over a natural riffle–pool sequence: a computational study. Earth Surface Processes and Landforms 28, 689-705. doi:10.1002/esp.466.

Carbonneau, P.E., Lane, S.N., Bergeron, N., 2006. Feature based image processing methods applied to bathymetric measurements from airborne remote sensing in fluvial environments. Earth Surface Processes and Landforms 31, 1413-1423. doi:10.1002/esp.1341.

Carley, J.K., Pasternack, G.B., Wyrick, J.R., Barker, J.R., Bratovich, P.M., Massa, D.A., Reedy, G.D., Johnson, T.R., 2012. Significant decadal channel change 58-67 years post-dam accounting for uncertainty in topographic change detection between contour maps and point cloud models. Geomorphology, doi:10.1016/j.geomorph.2012.08.001.

Carling, P.A., 1991. An appraisal of the velocity-reversal hypothesis for stable pool-riffle sequences in the River Severn, England. Earth Surface Processes and Landforms 16(1), 19-31.

Clifford, N.J., Richards, K.S., 1992. The reversal hypothesis and the maintenance of riffle–pool sequences: a review and field appraisal In Carling, P.A., Petts, G.E. (Eds.) Lowland Floodplain Rivers: Geomorphological Perspectives. John Wiley and Sons Ltd., Chichester, UK, pp. 43-70.

Elkins, E.E., Pasternack, G.B., Merz, J.E., 2007. The use of slope creation for rehabilitating incised, regulated, gravel-bed rivers. Water Resources Research 43, W05432. doi:10.1029/2006WR005159.

Hilldale, R.C., Raff, D., 2008. Assessing the ability of airborne LiDAR to map river bathymetry. Earth Surface Processes and Landforms 33, 773-783. doi:10.1002/esp.1575.

Jackson, J.R., Pasternack, G.B., Wyrick, J.R., 2013. Substrate of the Lower Yuba River. Prepared for the Yuba Accord River Management Team. University of California at Davis Technical Report, Davis, CA.

Jackson, W.L., Beschta, R.L., 1982. A model of two-phase bedload transport in an Oregon coast range stream. Earth Surface Processes and Landforms 7(6), 517-527.

Keller, E.A., 1969. Form and fluvial processes of Dry Creek, near Winters, California. M.S. Thesis, University of California at Davis.

Keller, E.A., 1971. Areal sorting of bed-load material: the hypothesis of velocity reversal. Geological Society of America Bulletin 82, 753-756.

Keller, E.A., 1972. Areal sorting of bed-load material: the hypothesis of velocity reversal: Reply. Geological Society of America Bulletin 83, 915-918.

Keller, E.A., Florsheim, J.L., 1993. Velocity-Reversal Hypothesis - a Model Approach. Earth Surface Processes and Landforms 18(8), 733-740.

Lisle, T.E., 1979. A sorting mechanism for a riffle–pool sequence. Geological Society of America Bulletin 90(7 Part II), 1142-1157.

Lisle, T.E., Nelson, J.M., Pitlick, J., Madej, M.A., Barkett, B.L., 2000. Variability of bed mobility in natural, gravel-bed channels and adjustments to sediment load at local and reach scales. Water Resources Research 36(12), 3743-3755. doi:10.1029/2000WR900238.

MacVicar, B.J., Rennie, C.D., Roy, A.G., 2010. Discussion of “Unifying criterion for the velocity reversal hypothesis in gravel-bed rivers” by D. Caamaño, P. Goodwin, J.M.

Buffington, J.C.P. Liou, and S. Daley-Laursen. Journal of Hydraulic Engineering 136, 550-552.

MacWilliams, M.L., Wheaton, J.M., Pasternack, G.B., Kitanidis, P.K., Street, R.L., 2006. The flow-convergence routing hypothesis for riffle–pool maintenance in alluvial rivers. Water Resources Research 42, W10427. doi:10.1029/2005WR004391.

Manwaring, M., Cepello, S., Kennedy, S., Pasternack, G.B. 2009. Spawning riffle gravel supplementation for anadromous spring-run Chinook salmon and steelhead. Waterpower XVI, July 27-30, Spokane, WA. p. 1-18.

Marcus, W.A., Fonstad, M.A., 2008. Optical remote mapping of rivers at sub-meter resolutions and watershed extents. Earth Surface Processes and Landforms 33, 4-24. doi:0.1002/esp.1637.

Milan, D.J., Heritage, G.L., Large, R.G., Fuller, I.C., 2011. Filtering spatial error from DEMs: implications for morphological change estimation. Geomorphology 125, 160-171.

Moir, H.J., Pasternack, G.B., 2008. Interactions between mesoscale morphologic units, stream hydraulics and Chinook salmon (*Oncorhynchus tshawytscha*) spawning habitat on the Lower Yuba River, California. Geomorphology 100, 527-548.

Murray, A.B., 2003. Contrasting the goals, strategies, and predictions associated with simplified numerical models and detailed simulations. In: Prediction in Geomorphology, Wilcock, P.R., Iverson, R.M. (Eds). American Geophysical Union, Washington, DC, pp. 151-165.

Nelson, P.A., Bellugi, D., Dietrich, W.E., in press. Delineation of river bed-surface patches by clustering high-resolution spatial grain size data. Geomorphology. doi:10.1016/j.geomorph.2012.06.008.

Osterkamp, W.R., Lane, L.J., Foster, G.R., 1983. An analytical treatment of channel-morphology relations. U.S. Geological Survey Professional Paper 1288, Washington, DC.

Pasternack, G.B., 2011. 2D Modeling and Ecohydraulic Analysis. Createspace, Seattle, WA.

Pasternack, G.B. Senter, A.E., 2011. 21st Century instream flow assessment framework for mountain streams. California Energy Commission, PIER, Sacramento, CA.

Pasternack, G.B., Brown, R.A., 2013. Ecohydraulic Design of Riffle–Pool Relief and Morphological-Unit Geometry in Support of Regulated Gravel-Bed River Rehabilitation. In: Maddock, I., Harby, A., Kemp, P., Wood, P. (Eds.) Ecohydraulics: an integrated approach. John Wiley and Sons Ltd., Chichester, UK.

Pasternack, G.B., Wang, C.L., Merz, J.E., 2004. Application of a 2D hydrodynamic model to reach-scale spawning gravel replenishment on the lower Mokelumne River, California. River Research and Applications 20(2), 205-225.

Pasternack, G.B., Gilbert, A.T., Wheaton, J.M., Buckland, E.M., 2006. Error Propagation for Velocity and Shear Stress Prediction Using 2D Models For Environmental Management. Journal of Hydrology 328, 227-241.

Pasternack, G.B., Bounrisavong, M.K., Parikh, K.K., 2008. Backwater control on riffle-pool hydraulics, fish habitat, and sediment transport regime in gravel-bed rivers. Journal of Hydrology 357(1-2), 125-139. doi:10.1016/j.jhydrol.2008.05.014.

Pasternack, G.B., Tu, D., Wyrick, J.R., 2013. Chinook Adult Salmon Spawning Physical Habitat of the Lower Yuba River. Prepared for the Yuba Accord River Management Team. University of California, Davis.

Repetto, R., Tubino, M., Paola, C., 2002. Planimetric instability of channels with variable width. Journal of Fluid Mechanics 457, 79-109.

Richards, K.S., 1976. The morphology of riffle–pool sequences. Earth Surface Processes and Landforms 1, 71-88.

Sawyer, A.M., Pasternack, G.B., Moir, H.J., Fulton, A.A., 2010. Riffle–pool maintenance and flow convergence routing observed on a large gravel-bed river. Geomorphology 114, 143-160. doi:10.1016/j.geomorph.2009.06.021.

Smart, G.M., 1999. Turbulent velocity profiles and boundary shear in gravel bed rivers. Journal of Hydraulic Engineering 125, 106-116.

Thompson, D.M., 2002. Geometric adjustment of pools to changes in slope and discharge: a flume experiment. Geomorphology 46(3-4), 257-265.

Thompson, D.M., 2006. The role of vortex shedding in the scour of pools. Advances in Water Resources 29(2), 121-129.

Thompson, D.M., Hoffman, K.S., 2001. Equilibrium pool dimensions and sediment-sorting patterns in coarse-grained, New England channels. Geomorphology 38(3-4), 301-316.

Thompson, D.M., Wohl, E.E., Jarret, R.D., 1999. Velocity reversals and sediment sorting in pools and riffles controlled by channel constrictions. Geomorphology 27(3-4), 229-241.

Warrick J.A., Rubin, D.M. Ruggiero, P., Harney, J., Draut, A.E., Buscombe, D., 2009. Cobble Cam: grain-size measurements of sand to boulder from digital photographs and autocorrelation analyses. Earth Surface Processes and Landforms 34 (13), 1811-1821.

Wheaton, J.M., 2008. Uncertainty in morphological sediment budgeting of rivers. Ph.D. Thesis, University of Southampton, Southampton, UK.

Wheaton, J.M., Pasternack, G.B., Merz, J.E., 2004. Spawning Habitat Rehabilitation - II. Using hypothesis development and testing in design, Mokelumne River, California, U.S.A. International Journal of River Basin Management 2(1), 21-37.

Wheaton, J. M., Brasington, J., Darby, S., Merz, J. E., Pasternack, G. B., Sear, D. A., Vericat, D. 2010. Linking geomorphic changes to salmonid habitat at a scale relevant to fish. River Research and Applications 26:469-486.

White, J.Q., Pasternack, G.B., Moir, H.J., 2010. Valley width variation influences riffle–pool location and persistence on a rapidly incising gravel-bed river. Geomorphology 121, 206-221. doi:10.1016/j.geomorph.2010.04.012.

Whiting, P.J., Deitrich, W.E., 1991. Convective accelerations and boundary shear stress over a channel bar. Water Resources Research 27(5), 783 – 796.

Wilcock, P.R., Barta, A.F., Shea, C.C., Kondolf, G.M., Matthews, W.V.G., Pitlick, J.C., 1996. Observations of flow and sediment entrainment on a large gravel-bed river. Water Resources Research 32, 2897–2909.

Williams, G.P., 1986. River meanders and channel size. Journal of Hydrology 88, 147-164.

Woodsmith, R.D., Hassan, M.A., 2005. Maintenance of an obstruction-forced pool in a gravel-bed channel: streamflow, channel morphology, and sediment transport. In: Garcia, C., Batalla, R.J. (Eds.), Catchment Dynamics and River Processes: Mediterranean and Other Climate Regions. Development in Earth Surface Processes 7. Elsevier, Amsterdam, The Netherlands, pp. 169-196.

Wu, F.C., Yeh, T.H., 2005. Forced bars induced by variations of channel width: implications for incipient bifurcation. Journal of Geophysical Research: Earth Surface (2003-2012) 110(F2), 1-22.

Xu, J., 2004. Comparison of hydraulic geometry between sand- and gravel-bed rivers in relation to channel pattern discrimination. Earth Surface Processes and Landforms 29, 645-657. doi:10.1002/esp.1059.

List of Figures

Fig. 3. Velocity results rasters at 0.42 m^3/s for the original Dry Creek, no pool, and 10% and 30% width expansions.

Fig. 4. Velocity results rasters at 17.0 m^3/s for the original Dry Creek, no pool, and 10% and 30% width expansions.

Fig. 5. Velocity–discharge and Shields stress–discharge curves for the original Dry Creek topography, no pool, and the 10% and 30% width expansions.

Fig. 6. Bar graph of Shields stress values averaged along the pool and riffle cross section. Percentage is based on the wetted width of each cross section.

Fig. 7. Applying the Caamaño Criterion to each topographic model at 17.0 m^3/s discharge. B_r and B_p are riffle and pool water surface widths, respectively, D_z is residual pool depth, and h_{Rt} is riffle thalweg depth.

Table 1
Summary of pool modification geometry; pool experiment attributes are volume, cross-sectional area, and width for each design; cross-sectional area based on total available up to elevation 27.7 m

	Pool width		Pool cross section		Volume cut / filled (- / +)
Terrain	[m]	% change	[m^2]	% change	[m^3]
DC	9.3	0.0	14.0	0.0	0.0
NP	9.3	0.0	13.1	-6.5	25.2
WE10	10.2	10.0	15.6	10.9	-25.2
WE15	10.6	15.0	15.9	13.5	-34.3
WE20	11.1	20.0	16.3	15.9	-40.4
WE25	11.6	25.0	17.3	22.9	-76.8
WE30	12.1	30.0	17.2	22.5	-78.1

Table 2
Mean cross section velocity

Discharge (m^3/s)	DC Velocity (m/s)		NP Velocity (m/s)		WE10 Velocity (m/s)		WE15 Velocity (m/s)		WE20 Velocity (m/s)		WE25 Velocity (m/s)		WE30 Velocity (m/s)	
	Pool	Riffle	Pool	Riffle	Pool	Riffle	Pool	Riffle	Pool	Riffle	Pool	Riffle	Pool	Riffle
0.42	0.14	0.28	0.20	0.30	0.14	0.28	0.14	0.28	0.13	0.28	0.12	0.28	0.12	0.28
0.96	0.25	0.40	0.34	0.41	0.24	0.39	0.24	0.39	0.24	0.42	0.23	0.42	0.23	0.42
4.50	0.67	0.71	0.78	0.72	0.60	0.70	0.57	0.69	0.59	0.73	0.57	0.73	0.57	0.73
8.50	0.95	0.90	1.02	0.91	0.79	0.89	0.79	0.89	0.75	0.89	0.72	0.89	0.73	0.89
17.0	1.26	1.19	1.38	1.21	1.01	1.12	1.01	1.12	0.99	1.12	0.97	1.12	0.97	1.12

Table 3
Mean Shields stress (τ^*) at the pool and riffle for each discharge and terrain; pool D_{50} equals 10 mm and riffle D_{50} equals 32 mm

Discharge	DC		NP		WE10		WE15		WE20		WE25		WE30	
[cms]	Pool	Riffle	Pool	Riffle	Pool	Riffle	Pool	Riffle	Pool	Riffle	Pool	Riffle	Pool	Riffle
0.42	0.003	0.006	0.008	0.007	0.003	0.006	0.003	0.006	0.003	0.006	0.003	0.006	0.003	0.006
0.96	0.010	0.010	0.019	0.010	0.009	0.009	0.009	0.009	0.009	0.010	0.008	0.010	0.008	0.010
4.50	0.057	0.023	0.080	0.023	0.049	0.023	0.043	0.022	0.046	0.023	0.040	0.023	0.040	0.023
8.50	0.11	0.032	0.13	0.033	0.076	0.032	0.074	0.032	0.068	0.032	0.062	0.032	0.063	0.032
17.0	0.17	0.048	0.21	0.049	0.12	0.045	0.12	0.045	0.11	0.045	0.10	0.045	0.10	0.045

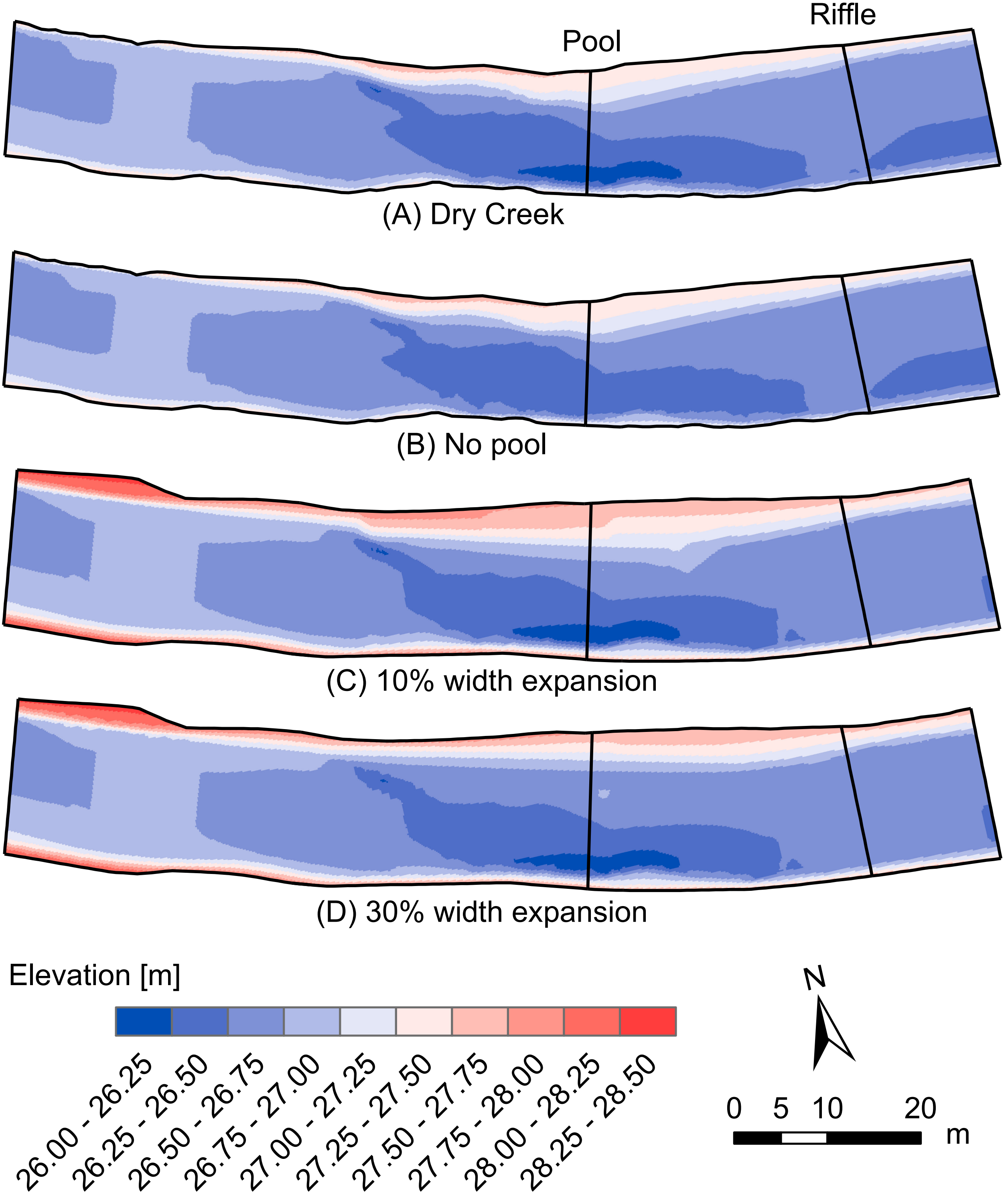
Riffle
Pool
(A) Dry Creek
(B) No pool
(C) 10% width expansion
(D) 30% width expansion
Elevation [m]
26.00 - 26.25
26.25 - 26.50
26.50 - 26.75
26.75 - 27.00
27.00 - 27.25
27.25 - 27.50
27.50 - 27.75
27.75 - 28.00
28.00 - 28.25
28.25 - 28.50
N
0 5 10 20
m

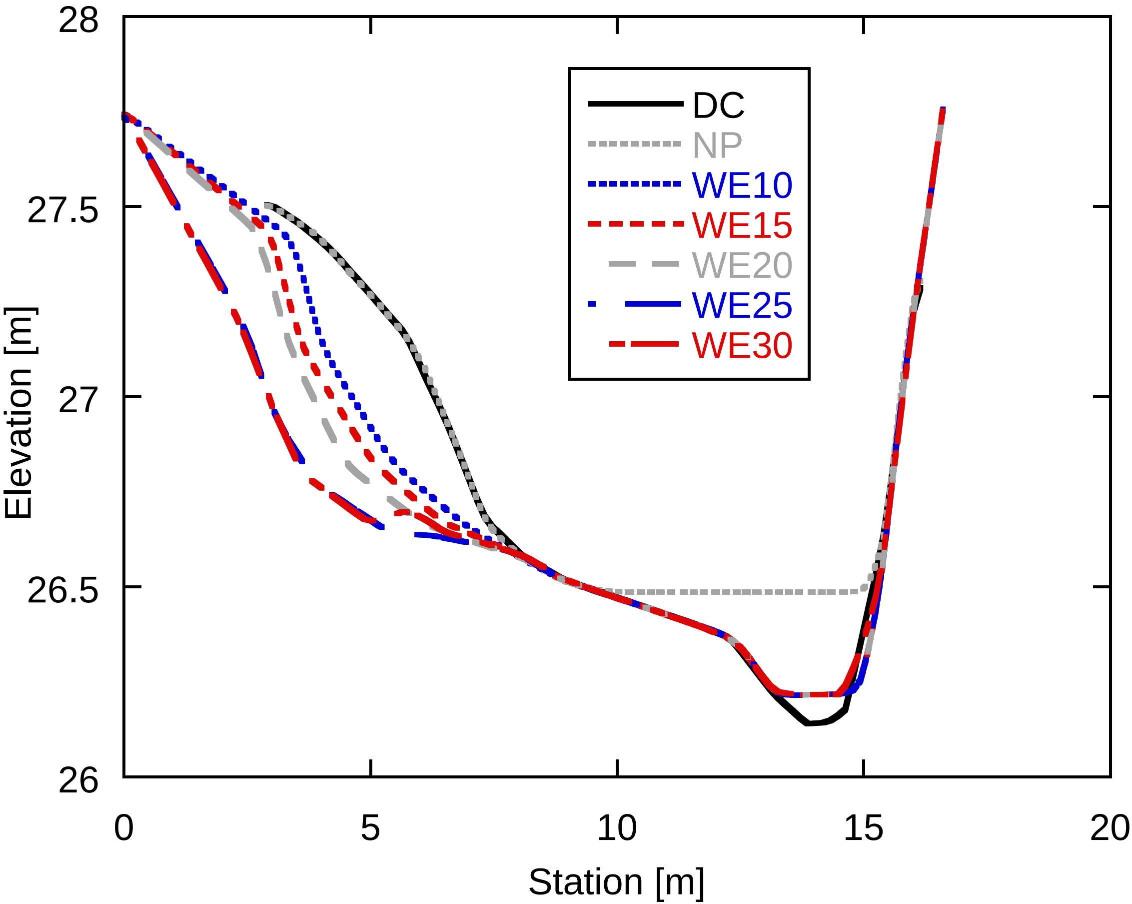

28
27.5
27
26.5
26
0
5
10
15
20
Station [m]
Elevation [m]
DC
NP
WE10
WE15
WE20
WE25
WE30

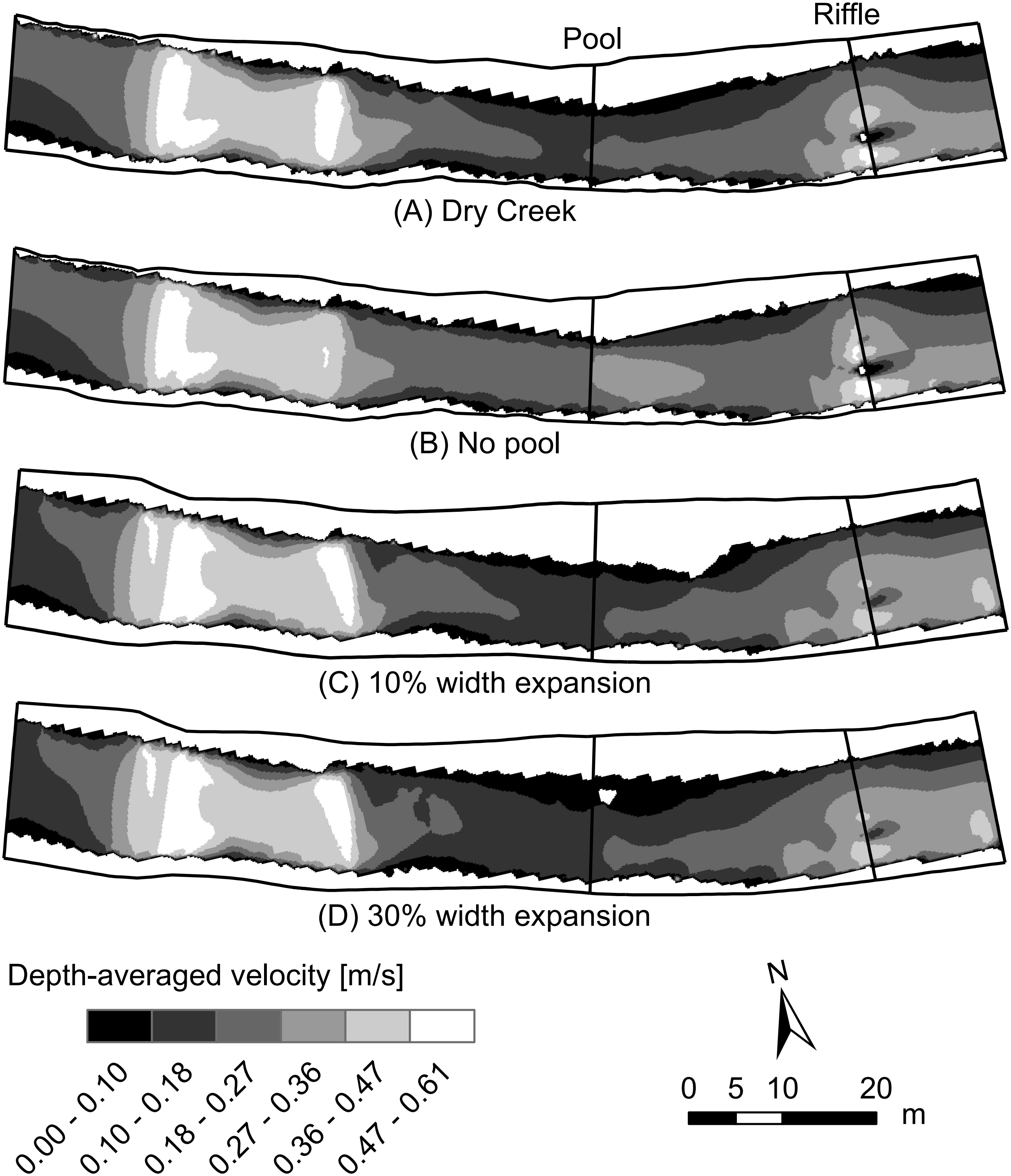
Pool
Riffle
(A) Dry Creek
(B) No pool
(C) 10% width expansion
(D) 30% width expansion
Depth-averaged velocity [m/s]
0.00 - 0.10
0.10 - 0.18
0.18 - 0.27
0.27 - 0.36
0.36 - 0.47
0.47 - 0.61
N
0
5
10
20
m

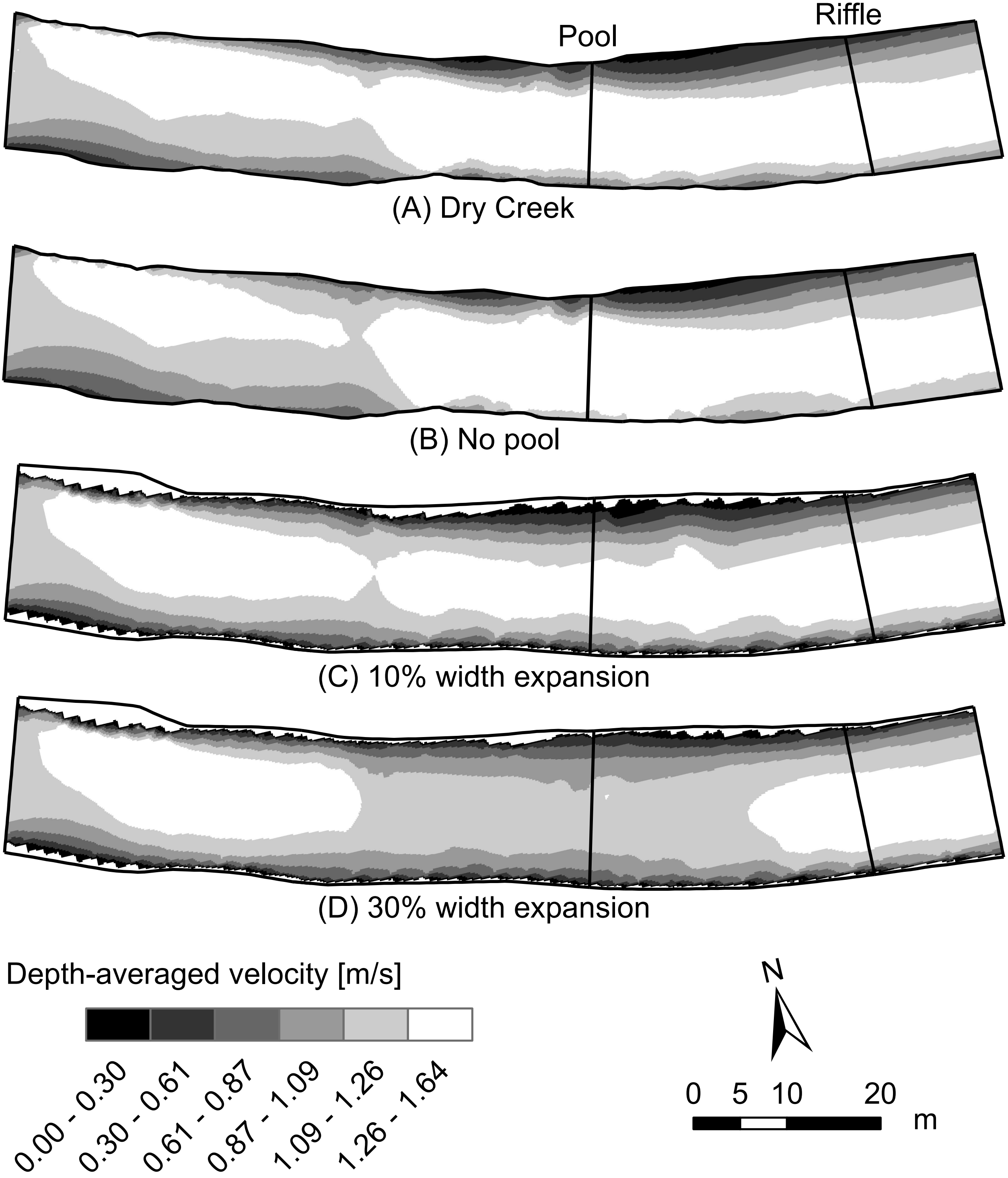

Pool
Riffle
(A) Dry Creek
(B) No pool
(C) 10% width expansion
(D) 30% width expansion
Depth-averaged velocity [m/s]
0.00 - 0.30
0.30 - 0.61
0.61 - 0.87
0.87 - 1.09
1.09 - 1.26
1.26 - 1.64
N
0
5
10
20
m

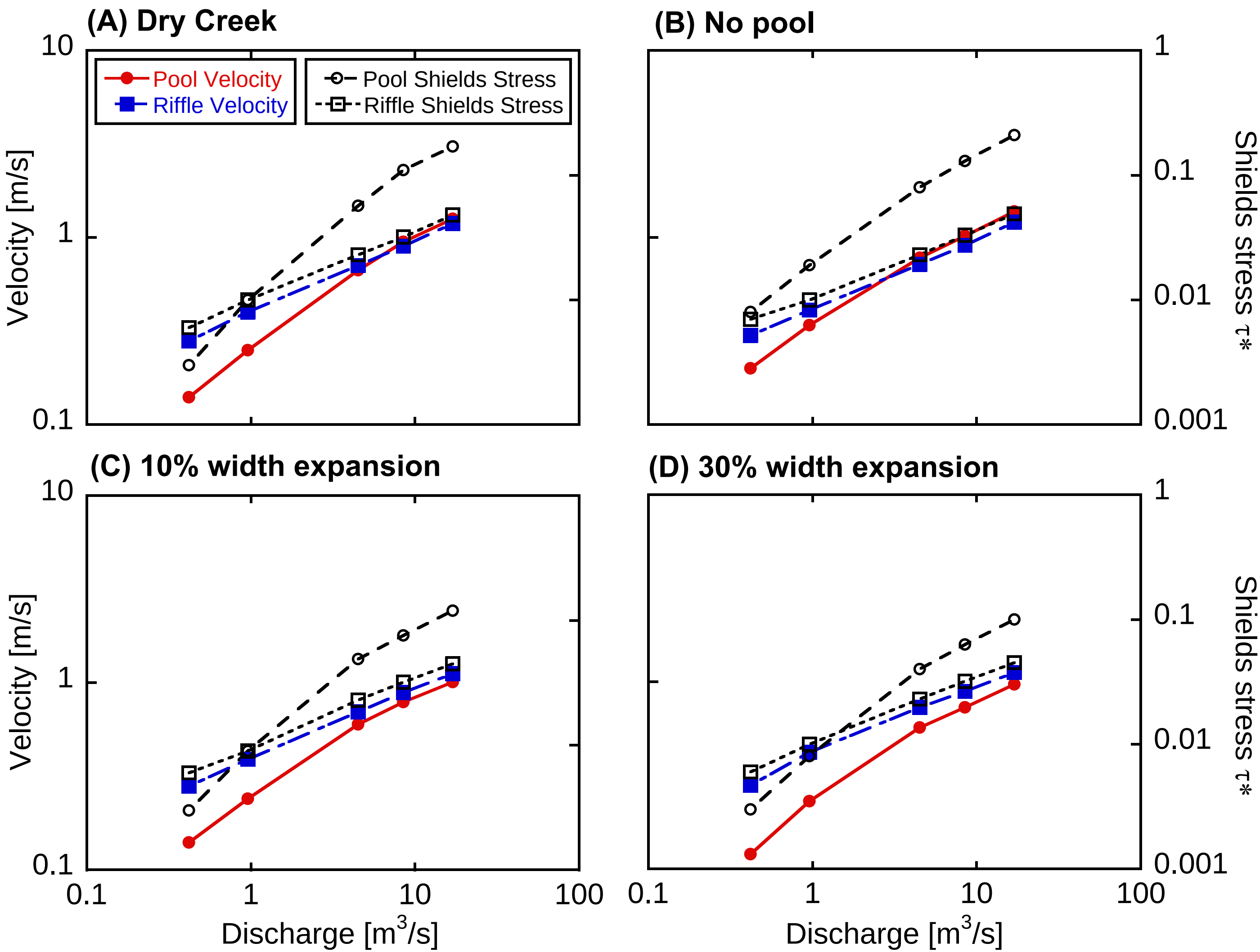
(A) Dry Creek
(B) No pool
(C) 10% width expansion
(D) 30% width expansion
Pool Velocity
Riffle Velocity
Pool Shields Stress
Riffle Shields Stress
Velocity [m/s]
Shields stress τ*
Discharge [m3/s]
10
1
0.1
0.01
0.001
100

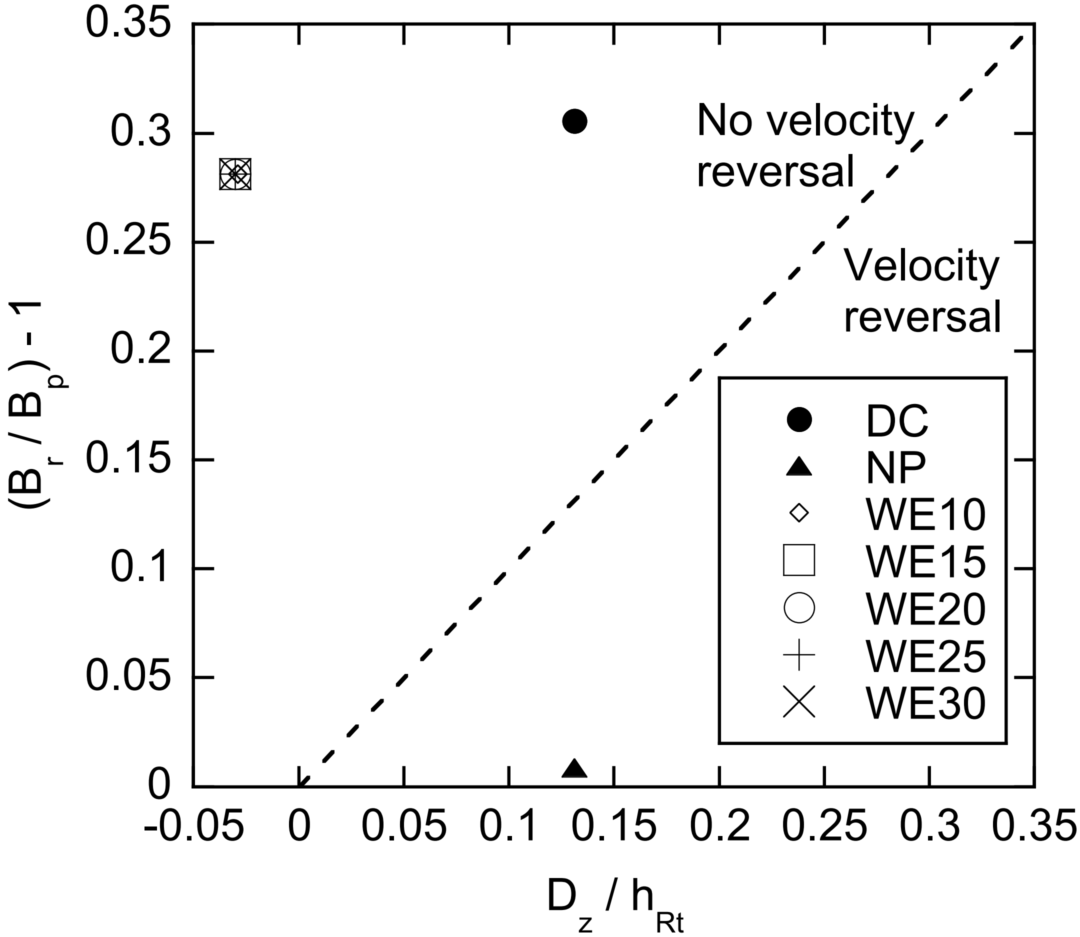

0.35
0.3
0.25
0.2
0.15
0.1
0.05
0
-0.05
0
0.05
0.1
0.15
0.2
0.25
0.3
0.35
$(B_r / B_p) - 1$
D_z / h_{Rt}
No velocity reversal
Velocity reversal
DC
NP
WE10
WE15
WE20
WE25
WE30

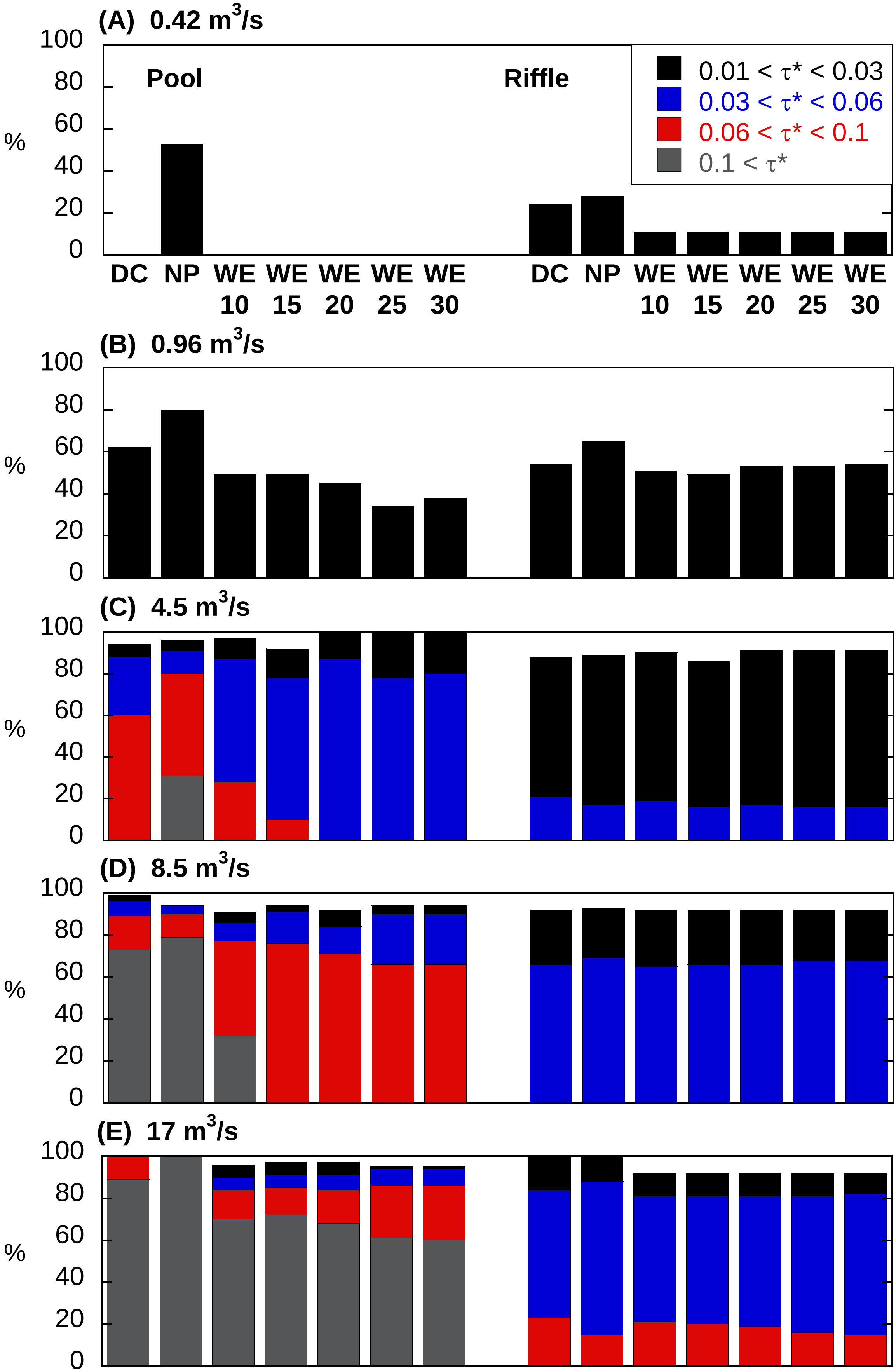

(A) 0.42 m3/s
Pool
Riffle
0.01 < τ* < 0.03
0.03 < τ* < 0.06
0.06 < τ* < 0.1
0.1 < τ*
%
100
80
60
40
20
0
DC
NP
WE 10
WE 15
WE 20
WE 25
WE 30
(B) 0.96 m3/s
(C) 4.5 m3/s
(D) 8.5 m3/s
(E) 17 m3/s